ISSN 2070-2051, Protection of Metals and Physical Chemistry of Surfaces, 2018, Vol. 54, No. 1, pp. 122–134. © Pleiades Publishing, Ltd., 2018.

PHYSICOCHEMICAL PROBLEMS OF MATERIALS PROTECTION

Application of Anise Extract for Corrosion Inhibition of Carbon Steel in CO_2 Saturated 3.0% NaCl Solution[1]

Amin Peimani[a] and Mojtaba Nasr-Esfahani[b, *]

[a]*Advanced Materials Research Center, Department of Materials Engineering, Najafabad Branch, Islamic Azad University, Najafabad, Iran*

[b]*Department of Chemistry, Najafabad Branch, Islamic Azad University, Najafabad, Iran*

**e-mail: m-nasresfahani@iaun.ac.ir*

Received February 23, 2016

Abstract—The corrosion inhibition of carbon steel in CO_2-saturated 3% NaCl solution by anise extract (AE) dissolved in ethylene glycol (EG) was studied using weight loss, electrochemical and surface analysis (AFM) techniques. Inhibition efficiency increased with increase in AE concentration and temperature, reaching maximum value of 93% at 400 ppm AE concentration. Polarization results show that AE functions as a mixed-type inhibitor. Corrosion inhibition is assumed to occur by physicochemical adsorption following Langmuir adsorption isotherm model. Morphological studies of the carbon steel electrode surface undertaken by AFM confirm the adsorption of the extract on the metal surface.

Keywords: carbon steel, CO_2 corrosion, inhibitor, anise extract, ethylene glycol

DOI: 10.1134/S2070205118010240

1. INTRODUCTION

Carbon steel is used in large quantity in marine applications, chemical processing, petroleum production and refining, construction and metal–processing equipment. They have been found to be very useful and economical [1, 2] despite its high corrosion susceptibility. These applications usually induce serious corrosive effect on equipment, tubes and pipelines made of iron and its alloys [3].

Carbon dioxide corrosion (CO_2) one of major problems in oil and gas industry and for several years causes losses amounting to millions of dollars per year [4]. In CO_2 corrosion, CO_2 dissolves and hydrates to form carbonic acid (H_2CO_3), which then dissociates into bicarbonate (HCO_3^-, carbonate (CO_3^{2-}) and hydrogen ions [5, 6]. Aqueous carbon dioxide (carbonic acid) is corrosive and corrodes the carbon steel pipelines. Carbon dioxide corrosion has been of interest to researchers in oil industries for many years and there exists many theories about the mechanism of CO_2 corrosion [7, 8]. The presence of CO_2 increases the rate of corrosion of carbon steel in aqueous solutions primarily by increasing the rate of the hydrogen evolution reaction. In strong acids, which are fully dissociated, the rate of hydrogen evolution occur according Eq. (1) and cannot exceed the rate at which H^+ ions are transported to the surface from the bulk solution (mass transfer limit). In CO_2 solutions, where tiypically pH > 4, this limiting flux of H^+ ions is small; therefore, it is the presence of H_2CO_3 that enables hydrogen evolution at a much higher rate. Thus, for pH > 4 the presence of CO_2 leads to a much higher corrosion rate than would be found in a solution of a strong acid at the same pH. The presence of H_2CO_3 can increase the corrosion rate in two different ways. Dissociation of H_2CO_3, as given by Eq. (2), serves as an additional source of H^+ ions [9].

$$2H^+ + 2e^- \rightarrow H_2, \quad (1)$$

$$H_2CO_3 \rightleftarrows H^+ + HCO_3^-, \quad (2)$$

$$Fe \rightarrow Fe^{2+} + 2e^-, \quad (3)$$

$$Fe^{2+} + CO_3^{2-} \rightarrow FeCO_3, \quad (4)$$

$$Fe^{2+} + 2HCO_3^{1-} \rightarrow Fe(HCO_3)_2, \quad (5)$$

$$Fe(HCO_3)_2 \rightarrow FeCO_3 + CO_2 + H_2O. \quad (6)$$

The anodic reaction is mainly the dissolution of iron (Eq. (3)) though it is maybe through several steps. During these corrosion processes, a corrosion scale ($FeCO_3$) would form on the surface of the carbon steels (Eqs. (4)–(6)) [10].

In order to reduce the corrosion of carbon steels in the oil and gas industry, inhibitors are frequently added to the produced fluid to control corrosion as an

[1] The article is published in the original.

economical and flexible method. Organic inhibitors such as imidazoline-based compounds have excellent inhibition ability in acidic media, they are widely used for protecting oil well, gas well or pipelines from CO_2 corrosion in the oil and gas industry [11]. However, the exorbitant cost, toxicity concerns and micelles formation by the long chain imidazolines based organic corrosion inhibitors are some of the drawbacks of this class of inhibitors. It is therefore highly desirable that new inhibitors for carbon steel that are non-toxic and environment-friendly be explored as a suitable replacement of the toxic ones. Natural products of plant origin has been advocated as an alternative to toxic organic and inorganic corrosion inhibitor given the facts that they are cheap, renewable, readily available, ecologically acceptable and environmentally friendly. More so, can be obtained by simple extraction procedures. The use of natural products as corrosion inhibitors in acidic media have been widely reported by several authors [12, 13]. These natural organic compounds are either synthesized or extracted from aromatic herbs, spices and medicinal plants. Presently, there is a scanty report on inhibitive effects of plant extracts on CO_2 corrosion of steel. Recently Singh et al. has reported on the inhibitive effect of extract of *Momordicacharantia* (Karela) seeds on carbon steel in CO_2-saturated 3.5% NaCl solution [14]. As our contribution to the growing interest on the use of bio-based corrosion inhibitor, we hereby report for the first time the inhibitive effect of anise extract on the CO_2 corrosion of the carbon steel.

Anise (*Pimpinellaanisum* L., *Apiaceae*) is a grassy annual plant with white flowers and small green to yellow seeds, grown inIran, Turkey, India, Egypt, and many other warm regions throughout the world [15]. It has been used as an aromatic herb and spice since Egyptian times and antiquity and has been cultivated throughout Europe [16].

In continuation of our ongoing programme to develop the inhibitive properties of green inhibitors in acidic media [17], we present here the inhibitive properties of extract of anise-fruits and its synergistic behavior with ethylene glycol, on CK10 carbon steel in CO_2-saturated 3.0% NaCl solutions using gravimetric and electrochemical techniques. A substantial number of studies concerning the inhibitor performance of glycols have been published [18, 19]. From an environmental point of view, glycols present a low toxicity; it is not surface active and bio accumulable. It is degradable and recycled in the process. It serves a dual function: hydrate prevention and corrosion control. The present work was undertaken with the aim of improving significantly the corrosion inhibition efficiency of a glycol-water system by addition of relatively low concentration of a bio-based green corrosion inhibitor.

2. EXPERIMENTAL METHODS

2.1. Preparation of Inhibitor

Pimpinellaanisum (anise) extract (AE) were obtained by percolation extraction using ethanol as solvent. The extraction cell (2.4 cm of internal diameter ×12 cm of height) was supplied with 10 g of ground anise previously packed in a filter paper extraction thimble. A solvent flask was filled with ethanol at the ratio 2 : 1 (v/w), which was recirculated through the system using a Masterflex pump (Barnant Company, model Solid State Speed Control, IL) adjusted to 0.2 g/s, making sure the raw material was covered with solvent all the time. The process was carried out without heating, for 72 h. The extract was concentrated initially using vacuum evaporator and finally by evaporation to dryness on a steam bath to obtain a solid residues devoid of the extractive solvent.

2.2. Materials Preparation

The test material selected for study was CK10 steel, its composition (wt %) was 0.1 C, 0.35Mn, 0.17 Si, 0.13 Cr, <0.04 Mo and Fe balance. Dish-shaped samples of 26 mm diameter and 3 mm diameter with total surface area measuring 13.1 cm^2 were used for weight-loss measurements. For electrochemical measurements, the metal samples were embedded in epoxy resin, leaving a geometrical surface area of 1 cm^2 exposed to the electrolyte. The surfaces were abraded with a series of silicon carbide papers, rinsed with distilled water and degreased in acetone and dried. Samples for AFM test had dimensions of 26 mm diameter and 2 mm thickness. The surface preparation method was similar to that described above.

An aqueous solution of 3.0% NaCl saturated with CO_2 at atmospheric pressure by continuous purging with carbon dioxide was used as test corrosive medium. Extracts of anise (AE) in concentrations ranging from 100 to 400 ppm was dissolved in 5 mL ethylene glycol (EG) and the obtained solution was added to CO_2-saturated 3.0% NaCl solution. The temperature was maintained within ±1°C in all the experiments by placing the cell on a thermostatted water bath. The solution was prepared from analytical grade chemicals using double distilled water.

2.3. Corrosion Weight-Loss Measurements

CK10 steel specimens were immersed in 500 mL of 3.0% NaCl CO_2-saturated solution with and without the anise extract at 25, 55 and 75°C for 24 h. The pH of the solution was 4.53. The coupons were then taken out of the test solution; the corrosion products were removed following ASTM G-31 standard practice procedure of cleaning of metals after weight loss tests, rinsed with distilled water, dried and weighed.

2.4. Electrochemical Measurement

For electrochemical measurement, the cell assembly consisted of CK10 steel as working electrode, a graphite rod of convenient area as counter electrode and a saturated calomel electrode (SCE) as a reference electrode. Electrochemical measurements were made using a PARSTAT 2273 electrochemical measurement system connected to a computer. Electrochemical impedance spectroscopy (EIS) was measured with perturbation amplitude of 5 mV at the corrosion potential and the frequency range was from 100 kHz to 10 mHz. The data were interpreted with Zview software. The potentiodynamic polarization study was from cathodic potential of −250 mV to anodic potential of + 250 mV with respect to the corrosion potential at a sweep rate of 1 mV/s. The stabilization of the open circuit potential was achieved at about 60 minutes after immersion. The linear Tafel segments of the anodic and cathodic curves were extrapolated to corrosion potential to obtain the corrosion current densities (i_{corr}). Each experiment was carried out three times to estimate reproducibility and average values of the electrochemical parameters are reported.

2.5. AFM Topographic Images and Force-Distance Curve Measurement

Atomic force microscopy (AFM) measurements were performed with a commercial AFM (dualscope-c26, Japan). The force curves were measured in contact mode using Si_3N_4 tips with spring constant of 0.02 N/m and the imaging process were performed in tapping mode using Si tips with spring constant of 3 N/m. The samples were immersed in test solutions for 24 h at 75°C, and then they were taken out of the electrolytes and slightly rinsed with distilled water, dried in a stream of air and submitted for AFM examination.

3. RESULTS AND DISCUSSION

3.1. Weight Loss Measurements

Weight loss measurements provide the most reliable results concerning the efficiency of a given inhibitor compound, such that the corresponding corrosion data obtained from the technique approaches service conditions more accurately than the data obtained with any other test methods. Table 1 presents the values of the corrosion rates (V) and the inhibition efficiency (IE_w), derived from weight-loss method at 25, 55 and 75°C in the absence and presence of EG and EG in combination with anise extract in CO_2-saturated 3.0% NaCl solution, the corrosion rate and inhibition efficiency were calculated using the following equations [20]:

$$V = \frac{8.76\times10^{7}\Delta W}{\rho A t}, \quad (7)$$

$$\theta = \frac{V_0 - V_{inh}}{V_0}, \quad (8)$$

$$IE_w(\%) = \theta\times100, \quad (9)$$

where A is the electrode surface area (cm^2), t represents the immersion time (h), ΔW is the weight loss (g). ρ corresponds to the steel density (kg/m^3), V_{inh} and V_0 are the corrosion rate (mm/yr) of steel with and without the additives, respectively. It is evident from Table 1 that the anise extract inhibitor when added to EG can inhibit CK10 steel from CO_2 induced corrosion effectively at 25, 55 and 75°C. The inhibition efficiency decreased with the addition of 5 mL EG, but it abruptly increased when 100 ppm AE was added to 5 mL EG. The highest IE of 96.7% was obtained in the presence of 5 ml EG in combination with 300 ppm AE. The inhibition efficiency of EG increased as the temperature increases. At 25, 55 and 75°C inhibition efficiencies of −20, −10 and 34% respectively were obtained in CO_2 saturated brine solution containing 5 mL EG. The presence of EG and anise extract leads to decrease of the corrosion rate. From Table 1, it could also be observed that IE decreased with increase in temperature for inhibiting solution comprised of EG in combination with the extract. For instance, at 25, 55 and 75°C inhibition efficiencies of 96.7, 92.5 and 86% respectively were obtained in CO_2 saturated brine solution containing 5 mL EG in combination with 300 ppm AE.

3.2. Potentiodynamic Polarization Measurements

In order to assess the ability of anise extract to function as inhibitor for pipeline steels, electrochemical experiments were conducted on CK10 carbon steel in CO_2-saturated 3.0% NaCl without, with EG and EG combined with selected concentrations (200 and 400 ppm) of anise extract at 25°C. Figure 1 shows the potentiodynamic polarization curves for the carbon steel, in CO_2-saturated brine solution containing different concentrations of anise extract at 25°C. As seen in Fig. 1, cathodic current increased with the addition of EG, but it abruptly decreased depending on anise extract concentration added to EG. The corrosion potential shift to negative values and the decrease of cathodic currents correlates well with the growth of inhibitor concentration. Practically parallel shift of cathode curves shows that the adsorption of anise extract compounds does not depend on potential in a wide range till −200 mV with respect to the corrosion potential and that in the cathode region molecules are not desorbed from the metal surface. Upon anodic polarization, the slope of the curves is sharply changed with respect to the blank due to the significant decrease of the anodic currents. More significant decrease of anode currents in comparison with cathode currents show that the studied compounds are

Table 1. Corrosion parameters obtained from weight-loss method for CK10 steel in 3.0% NaCl solution saturated with CO_2 with ethylene glycol contain various concentrations of anise extract at 25, 55 and 75°C for 24 h

Temperature, °C	Systems	Weight loss, mg cm^{-2} h^{-1}	θ	IE_W, %	Corrosion rate, mpy
25	3.0% NaCl	0.0959	–	–	42.1
	3.0% NaCl + 5 mL EG + 0 ppm AE	0.1150	–0.02	–20	50.8
	3.0% NaCl + 5 mL EG + 100 ppm AE	0.0096	0.900	90	4.2
	3.0% NaCl + 5 mL EG + 200 ppm AE	0.0064	0.933	93.3	2.8
	3.0% NaCl + 5 mL EG + 300 ppm AE	0.0032	0.967	96.7	1.4
	3.0% NaCl + 5 mL EG + 400 ppm AE	0.0064	0.933	93.3	2.8
55	3.0% NaCl	0.1278	–	–	56.2
	3.0% NaCl + 5 mL EG + 0 ppm AE	0.1406	–0.01	–10	62.1
	3.0% NaCl + 5 mL EG + 100 ppm AE	0.0134	0.895	89.5	5.9
	3.0% NaCl + 5 mL EG + 200 ppm AE	0.0128	0.900	90.0	5.6
	3.0% NaCl + 5 mL EG + 300 ppm AE	0.0096	0.925	92.5	4.2
	3.0% NaCl + 5 mL EG + 400 ppm AE	0.0128	0.900	90.0	5.6
75	3.0% NaCl	0.1598	–	–	70.2
	3.0% NaCl + 5 mL EG + 0 ppm AE	0.1054	0.034	34	29.1
	3.0% NaCl + 5 mL EG + 100 ppm AE	0.0265	0.834	83.4	11.7
	3.0% NaCl + 5 mL EG + 200 ppm AE	0.0246	0.846	84.6	10.8
	3.0% NaCl + 5 mL EG + 300 ppm AE	0.0224	0.860	86.0	9.8
	3.0% NaCl + 5 mL EG + 400 ppm AE	0.0249	0.844	84.4	11.0

inhibitors of the mixed type with the predominant influence on the anodic process.

Table 2 shows electrochemical parameters of the carbon dioxide corrosion of carbon steel, obtained from Tafel extrapolation method, such as corrosion current density (i_{corr}), corrosion potential (E_{corr}), cathodic Tafel's slope (β_c), anodic Tafel's slope (β_a) and inhibition efficiency, IE_p (%) for different concentrations of anise extract at temperatures 25–75°C. IE_p (%) was calculated as follows:

$$IE_p(\%) = \frac{100 \times \left[i^0_{corr} - i_{corr} \right]}{i^0_{corr}}, \quad (10)$$

where i^0_{corr} and i_{corr} are corrosion current densities without and inhibitor respectively determined by extrapolating the linear Tafel regions of the polarization curves to the E_{corr} [21]. It can be seen that anise extract inhibits the corrosion of the carbon steel to an appreciable extent and that the extent of inhibition is dependent on the inhibitor concentration at all temperatures.

Potentiodynamic studies showed that the activity of inhibitor is connected not only with the blocking of the metal surface as a result of adsorption of inhibitor's molecules, but also with a significant change of the mechanism of anodic and cathodic reactions. The change of polarization curves gives the evidence that the tested compounds inhibit one or more adjoining reactions on the electrode surface.

3.3. Electrochemical Impedance Measurements

Figure 2a shows Nyquist plots for carbon steel electrode in the CO_2 saturated 3.0% NaCl solution without inhibitor as well as in the presence of various concentrations of anise extract at 25°C. In the absence of inhibitor impedance diagram usually observed in CO_2 media [22, 23], consisting of a large capacitive loop at high frequency followed by a not well defined inductive one at low frequencies is observed. The slightly depressed nature of the semicircle which has the center below the real axis is the characteristic for solid electrodes that show frequency dispersion. Such frequency dispersion has been attributed to roughness and other inhomogeneties of the solid electrode. It is seen that the diameter of high-frequency semicircle grow upon the increase in the inhibitor's concentration. As usually indicated in the EIS study, the capacitive loop is related to the charge transfer process of carbon steel through adsorption of intermediate corrosion product [24]. In the conditions of our experiment in which we used laminar flow with a stirring rate of 500 rpm, we did not observe a straight line in the low frequency range (Warburg impedance). This indicates an insignificant level of a convective mass transport or mass transport limitations. Furthermore on the

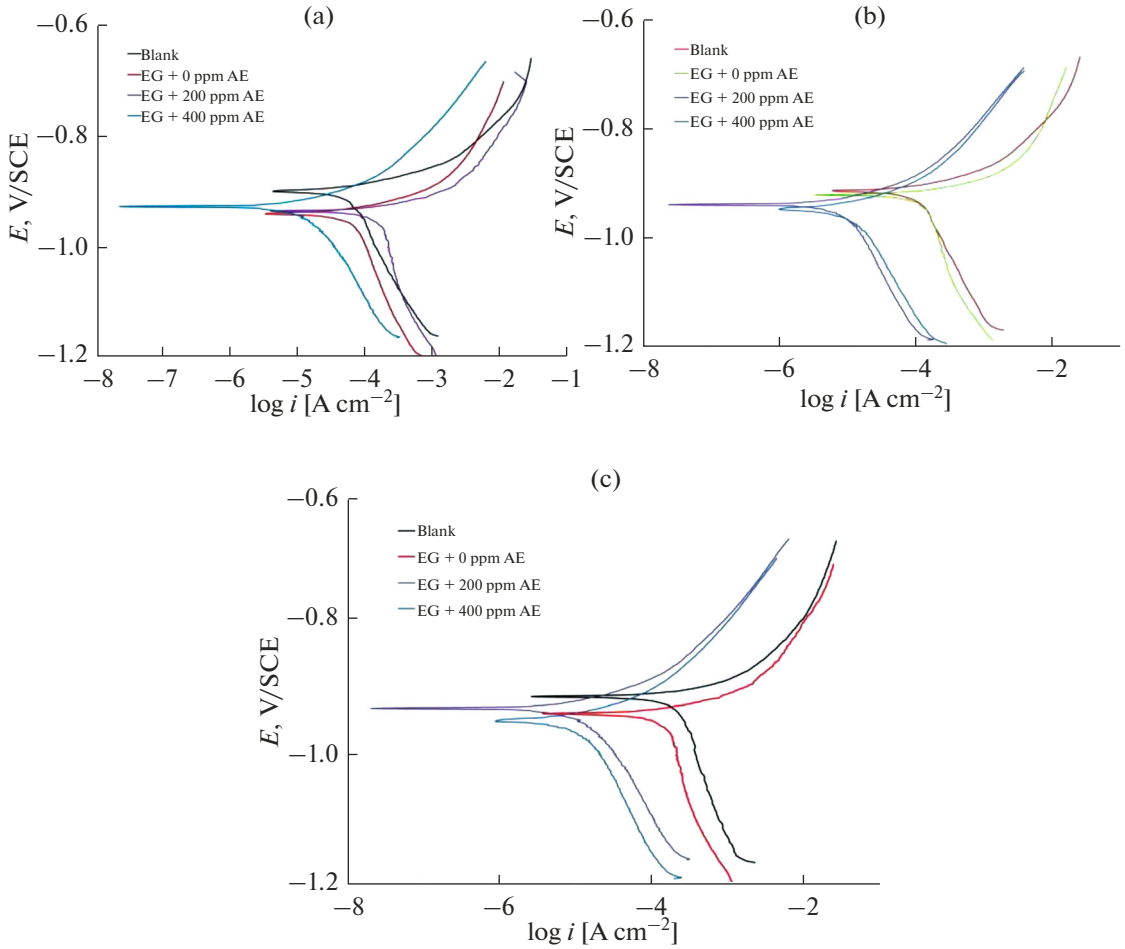

Fig. 1. Polarization curves of carbon steel in brine containing different concentration of anise extract at (a) 25; (b) 55 and (c) 75°C.

Bode graphs (Fig. 2b, 2c) there is only one maximum, which is sharply increased and is moved together with growth of concentration of anise extract in low-frequency area. These facts specify that the electrode reactions are controlled by charge transfer.

The impedance data for CK10 carbon steel in CO_2-saturated 3% NaCl in the absence and presence of the additives (EG and EG + anise extract) were analyzed using the equivalent circuit (EC) model shown in Fig. 3. The circuit is made up of hierarchical arrangement comprises of two stacked resistance-constant phase element (*CPE*) pairs, R_s as the solution resistance, R_{ct} and R_f as the charge transfer resistance and inhibitor film resistance respectively. The EC representing the interface phenomena is composed of elements describing the properties of the inhibitor exemplified by Q_f and R_f and those related to the corrosion process exemplified by Q_{dl} and R_{ct} on the carbon steel surface. Excellent fit with this model was obtained for all experimental data. The constant phase element (CPE) is used instead of capacitor to account for the roughness and inhomogeneities of the solid electrode [25]. The impedance, Z of CPE is given by:

$$Z_{CPE} = Y_0^{-1}(j\omega)^{-n}, \quad (11)$$

where Y_0 is the CPE constant and n the CPE exponent; $j = (-1)^{1/2}$ which is an imaginary number and ω is the angular frequency in rad/s.

The double layer capacitance was been estimated by using follows equation:

$$C_{dl} = Y_0(2\pi f_{max})^{n-1}, \quad (12)$$

where f_{max} is frequency at which the imaginary component of the impedance is maximum. The values of electrochemical impedance parameters derived from the Nyquist plots in the absence and presence of the additives are given in Table 3. Also presented in Table 3 is the inhibition efficiencies, $IE_A\%$, values of the tested inhibitors calculated from the R_{ct} values at different concentrations using the following equation:

Table 2. Potentiodynamic polarization parameters for CK10 carbon steel in 3% NaCl solutions saturated with CO_2 at pH 4.53 without and with inhibitors

Temperature, °C	Systems	$-E_{cor}$, mV	i_c, μA cm^{-2}	$-\beta_c$, mV/dec	$-\beta_a$, mV/dec	IE_p, %	mpy
25	3.0% NaCl	659	59.4	271	63	–	27.3
	3.0% NaCl + 5 mL EG + 0 ppm AE	699	70.1	322	86	–18	32.2
	3.0% NaCl + 5 mL EG + 200 ppm AE	677	15.2	218	110	74.4	6.9
	3.0% NaCl + 5 mL EG + 400ppm AE	694	4.2	200	96	92.8	1.9
55	3.0% NaCl	670	102	240	86	–	46.9
	3.0% NaCl + 5 mL EG + 0 ppm AE	679	112	384	85	–9.8	51.5
	3.0% NaCl + 5 mL EG + 200 ppm AE	696	9.4	230	88	90.8	4.3
	3.0% NaCl + 5 mL EG + 400 ppm AE	704	10.1	213	89	90.1	5.6
75	3.0% NaCl	668	236.7	430	79	–	108.9
	3.0% NaCl + 5 mL EG + 0 ppm AE	694	160.9	507	82	32.0	74.0
	3.0% NaCl + 5 mL EG + 200 ppm AE	686	12.4	170	85	94.7	5.7
	3.0% NaCl + 5 mL EG + 400 ppm AE	706	12.5	219	87	94.6	5.8

Table 3. Electrochemical impedance spectroscopy parameters for CK10 carbon steel in 3% NaCl solutions saturated with CO_2 at pH 4.53 without and with inhibitors

Temperature, °C	Systems	R_s, Ω cm^2	Y_f, μΩ s^n cm^{-2}	n_f	R_f, Ω cm^2	Y_{odl}, μΩ s^n cm^{-2}	n_{dl}	R_{ct}, Ω cm^2	C_{dl}, μΩ s^n cm^{-2}	IE_A, %
25	3.0% NaCl	4	1999	0.96	5	1154	0.93	195	1083	–
	3.0% NaCl + 5 mL EG + 0 ppm AE	8	45	0.94	1	1129	0.81	168	730	–16.1
	3.0% NaCl + 5 mL EG + 200 ppm AE	3	18	0.93	4	60	0.81	600	29	67.4
	3.0% NaCl + 5 mL EG + 400 ppm AE	9	54	0.76	33	27	0.85	2361	19	91.7
55	3.0% NaCl	5	1398	0.97	12	939	0.96	66	857	–
	3.0% NaCl + 5 mL EG + 0 ppm AE	5	580	0.84	60	184	0.95	59	224	–12
	3.0% NaCl + 5 mL EG + 200 ppm AE	4	42	0.75	10	137	0.83	1333	93	95.0
	3.0% NaCl + 5 mL EG + 400 ppm AE	5	57	0.83	16	136	0.83	978	92	93.2
75	3.0% NaCl	5	1650	0.96	6	1098	0.92	58	1004	
	3.0% NaCl + 5 mL EG + 0 ppm AE	7	1395	0.66	0	171	0.97	106	159	45
	3.0% NaCl + 5 mL EG + 200 ppm AE	5	1609	0.59	7	165	0.84	489	97	88.1
	3.0% NaCl + 5 mL EG + 400 ppm AE	6	47	0.81	12	142	0.84	952	99	93.9

$$IE_A\,(\%) = \left(1 - \frac{R_{ct}^0}{R_{ct}}\right) \times 100, \qquad (13)$$

where R_{ct}^0 and R_{ct} are the charge-transfer resistance values in the absence and presence of inhibitor, respectively. Results in the table show that R_{ct} values increased while C_{dl} values decreased in the presence of the additives compared to the blank which was more pronounced in the EG + anise extract inhibiting system at all temperatures studied. The increase in R_{ct} values indicates corrosion protection effect of the additives by virtue of adsorption of the inhibitor on the electrode surface which replaces the water molecules and hence decreasing the extent of dissolution reaction. On the other hand, the decrease in C_{dl} value of inhibited solution with respect to that of the blank solution is attributed to the decrease in dielectric constant and/or an increase in the double-layer thickness.

3.4. Adsorption Isotherm

The adsorption isotherms describe interaction of the inhibitor molecule with the active sites on the steel

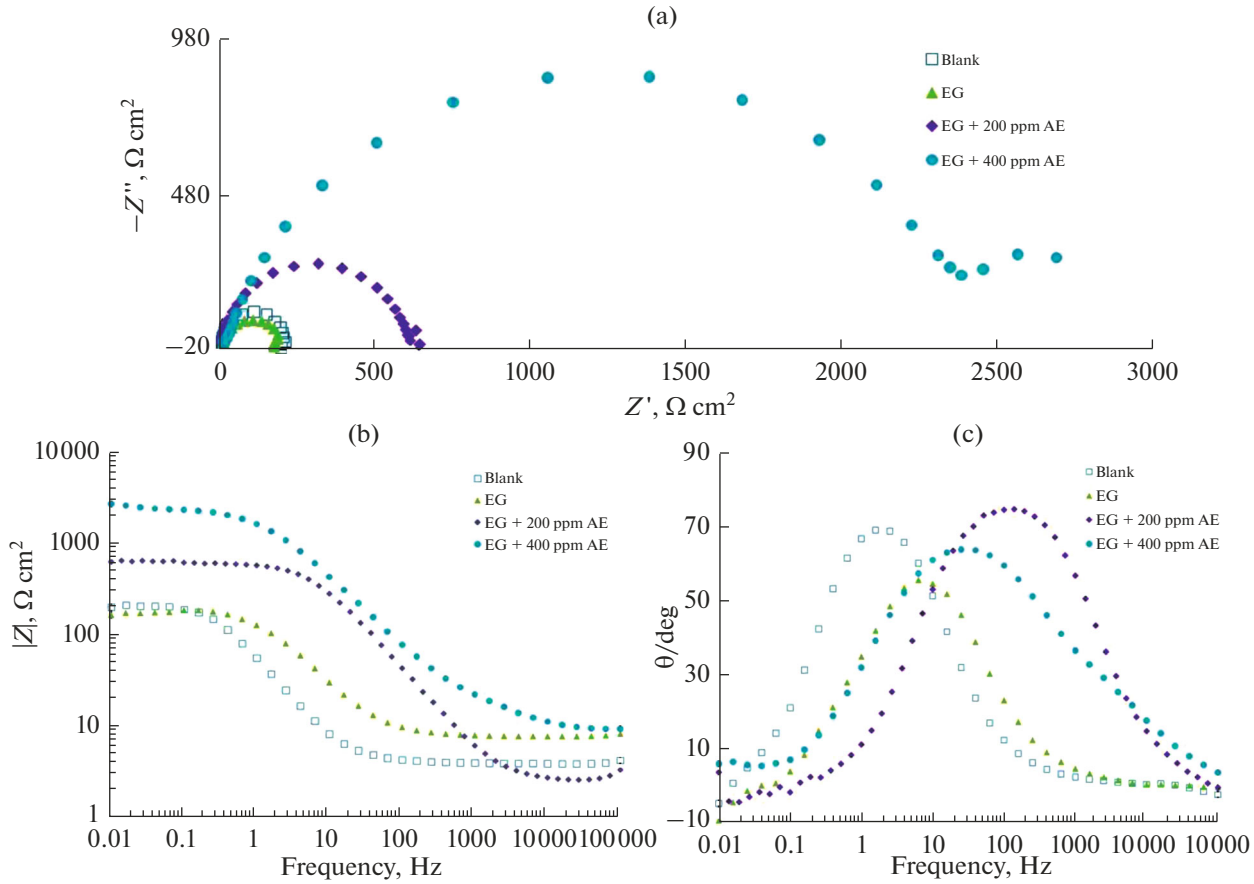

Fig. 2. Nyquist plots for carbon steel in CO_2 saturated brine containing: (a) 0, 200, 400 ppm, and blank at 25°C, (b and c) Bode plots for 0, 200, 400 ppm, and blank at 25°C.

surface. In order to obtain these isotherms, it was assumed that the corrosion process occurs only at the free active sites of the metal surface and the sites, covered by adsorbed molecules, have zero corrosion rates. The degree of surface coverage (θ) was calculated using Eq. (8) from the weight loss measurements. Attempts were made to fit surface coverage values (θ) to various adsorption isotherms and the correlation coefficient (R^2) was used to choose the isotherm that best fit the experimental data. The Langmuir isotherm was found to provide best description of the adsorption of anise extract on metal surface. Langmuir isotherm is characterized by:

$$\frac{\theta}{1-\theta} = K_{ads}C. \quad (14)$$

Rearranging gives:

$$\frac{C}{\theta} = \frac{1}{K_{ads}} + C, \quad (15)$$

where K_{ads} is the equilibrium constant of the adsorption-desorption process, C is the inhibitor concentration and θ is the degree of surface coverage.

Figure 4 depicts the plot of C/θ against C which is found to be straight line with slopes around unity. This suggests that the adsorption of anise extract on metal surface followed the Langmuir adsorption isotherm model. Adsorption parameters derived from the Langmuir isotherm are given in Table 4. K_{ads} values which usually indicate adsorption strength between the adsorbate and adsorbent is seen in Table 4 to increase with increase in temperature an indication that anise extract exhibits a stronger tendency to adsorb on steel

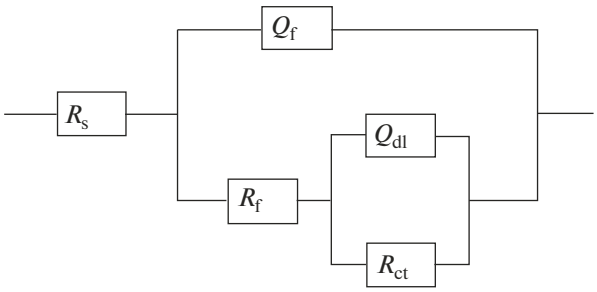

Fig. 3. Equivalent circuit model used to analyze the impedance data.

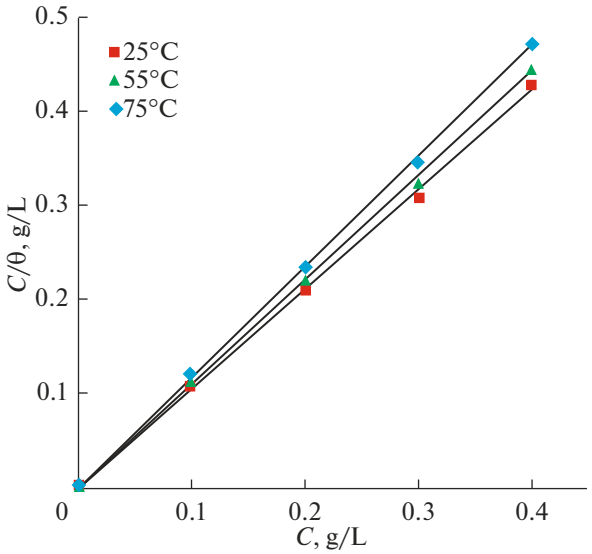

Fig. 4. Langmuir adsorption plots for CK10 carbon steel in CO_2-saturated brine at different temperatures.

surface with increase in solution temperature. The most important thermodynamic adsorption parameter, the free energy of adsorption (ΔG_{ads}) is related to the equilibrium constant of adsorption-desorption process, K_{ads}, by the following equation [26]:

$$K_{ads} = \left(\frac{1}{55.5}\right)\exp\left(-\frac{\Delta G_{ads}}{RT}\right), \quad (16)$$

where 55.5 is the concentration of water in mol/dm^3. The calculated values of standard free energy of adsorption (ΔG_{ads}) are also listed in Table 4. The negative values of ΔG_{ads} indicates the stability of the adsorbed layer on the steel surface and spontaneity of the adsorption process. The dependence of ΔG_{ads} on temperature can be explained by two cases as follows [27]:

(a) ΔG_{ads} may increase (becomes less negative) with the increase of temperature which indicates the occurrence of exothermic process.

(b) ΔG_{ads} may decrease (becomes more negative) with increasing temperature indicating the occurrence of endothermic process.

Table 4. Thermodynamic parameters for the adsorption of anise extract in CO_2 saturated brine solutions on the carbon steel at different temperatures

Temperature, °C	R^2	Slope	K_{ads}, L/mg	ΔG_{ads}, kJ/mol
25	0.998	1.048	254.5	23.7
55	0.997	1.101	4000	30.5
75	0.997	1.176	2174	28.9

Therefore, the decrease of ΔG_{ads} with temperature reveals that the inhibition of carbon steel by anise extract is an endothermic process. In an endothermic process adsorption was favorable with increasing reaction temperature due to the inhibitor adsorption on the steel surface [28]. It is suggestive that the mechanism of adsorption of the inhibitor on the carbon steel surface is mainly by a chemical adsorption mechanism. For physical adsorption, the inhibition efficiency is expected to decrease with increasing temperature, but for chemical adsorption, the inhibition efficiency is expected to increase with increasing temperature.

3.5. Effect of Temperature

The effect of temperature on the carbon steel in the absence of EG and AE and presence of EG and EG with 200 ppm AE in the CO_2 saturated solutions in the range of temperature 25–75°C was examined using the potentiodynamic polarization technique. Typical potentiodynamic polarization curves for the different systems studied are shown in Fig. 5. Increase in temperature is observed to accelerate both the anodic and cathodic reactions in the absence and presence of anise extract, as evident in the increased i_{corr} with temperature (Table 2). This is due to the acceleration of all the processes involved in corrosion: electrochemical, chemical, transport, etc. with increase in temperature [29].

Arrhenius-type dependence is observed between corrosion rate (V) and temperature often expressed as in Eq. (17):

$$V = A\exp\left(-\frac{E_a^*}{RT}\right), \quad (17)$$

where V is the corrosion rate, E_a^* is the apparent activation energy, R is the molar gas constant, T is the absolute temperature, and A is the frequency factor.

Figure 6 depicts an Arrhenius plot (logarithm of V against the reciprocal of temperature ($1/T$)) for CK10 carbon steel in the absence and presence of EG and EG in combination with 300 ppm AE in the CO_2-saturated solutions in the range of temperature 25–75°C. Linear plots were obtained and the values of activation energy (E_a) obtained from the slope of the plot are given in Table 5. In the absence of EG and anise extract, the activation energy obtained was 8.7 kJ mol^{-1} for CK10 carbon steel in the CO_2-saturated solution. These values are slightly higher than that of aqueous diffusion coefficient and indicate a mixed interfacial reaction/diffusion control [30]. The presence of EG was observed to increase the activation to 16.1 kJ mol^{-1} for the corrosion of CK10 carbon steel in the CO_2-saturated solution. The presence of EG and 300 ppm anise extract was observed to increase the activation to 33.1 kJ mol^{-1}. The increase in activation energy after

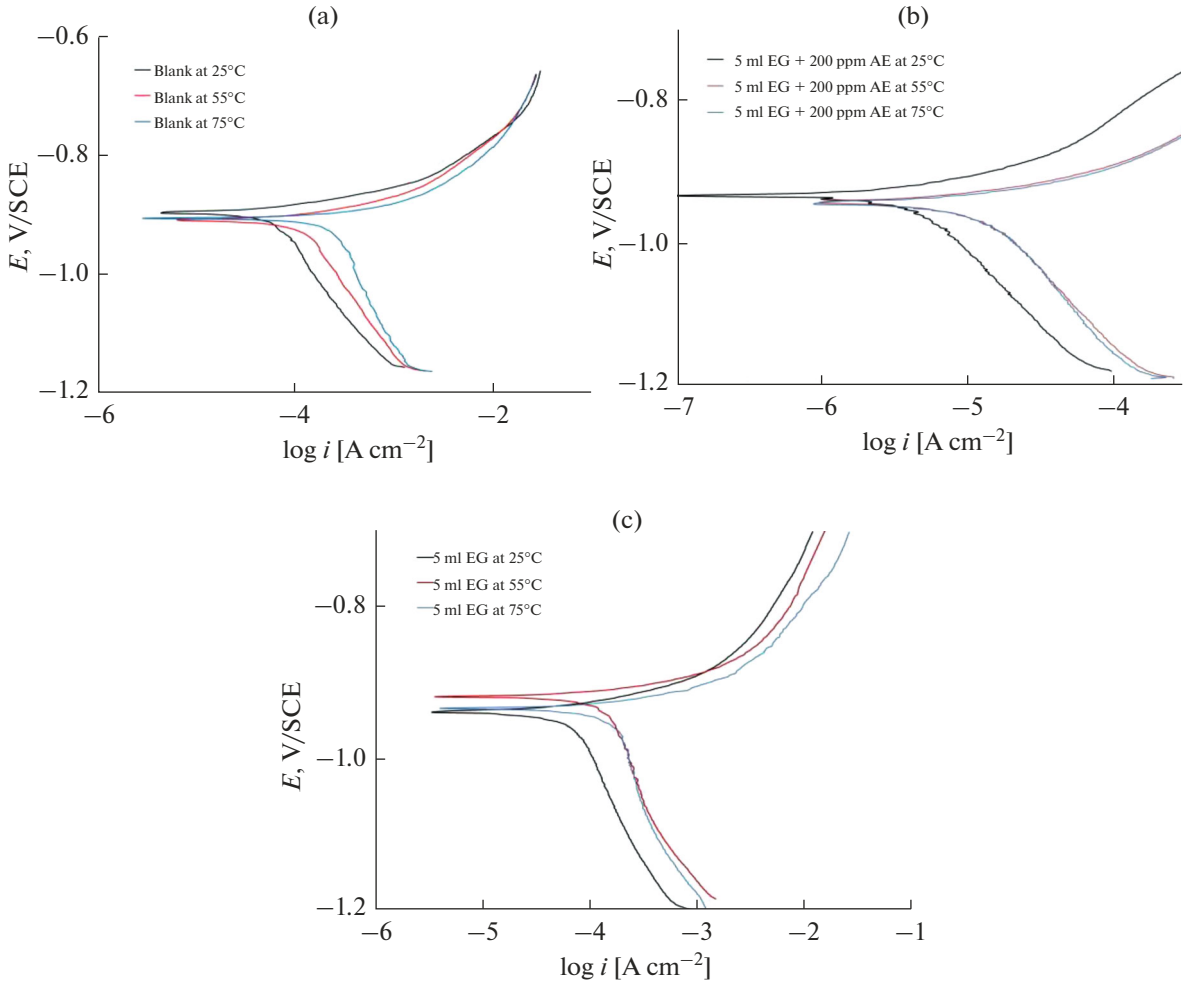

Fig. 5. Polarization curves for CK10 carbon steel in CO_2-saturated brine solution in the absence of inhibitor (a) in the presence of EG without AE (b) and in the presence of EG with 200 ppm AE (c) at 25, 55, and 75°C.

the addition of the inhibitor in comparison to the blank solution coupled with a decrease in inhibition efficiency with temperature rise has often been attributed from literature report to the formation of an inhibitor film by physicochemical adsorption mechanism [31, 32]. The value of E_a (33.1 kJ mol^{-1}) obtained for 300 ppm anise extract – EG mixtures fits into the range of values (30–50 kJ mol^{-1}) reported for adsorption of organic molecules on carbon steel surface.

The enthalpy of activation (ΔH^*) and the entropy of activation (ΔS^*) for the corrosion of CK10 carbon steel in CO_2-saturated brine solution were obtained by applying the transition-state equation [33]:

$$\log\frac{V}{T} = \left[\left(\log\frac{R}{hN}\right) + \left(\frac{\Delta S^*}{2.303R}\right)\right] - \frac{\Delta H^*}{2.303RT}, \quad (18)$$

where h is the Planck's constant and N is the Avogadro's number. Figure 7 shows a plot of $\log(V/T)$ versus $1/T$. Straight lines are obtained from which the values of ΔH^* and ΔS^* were obtained from the slope and

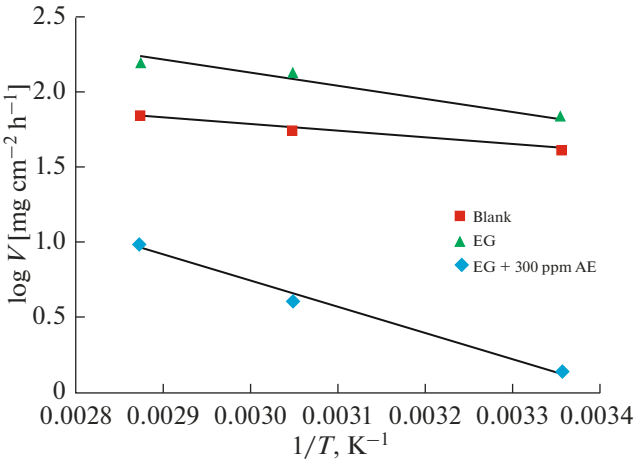

Fig. 6. Arrhenius plot of variation of ($\log V$) vs. ($1/T$) for dissolution of CK10 carbon steel in CO_2-saturated brine solution in absence and presence of 300 ppm of anise extract.

Table 5. The values of activation parameters for CK10 carbon steel in CO_2 saturated brine solutions in the absence and the presence of different concentrations of AE

System	E_a, kJ/mol	ΔH^*, kJ/mol	ΔS^*, J/mol K
3.0% NaCl	8.7	6.1	3.9
3.0% NaCl + 5 mL EG + 0 ppm AE	16.1	13.7	32.8
3.0% NaCl + 5 mL EG + 300 ppm AE	33.1	31.1	48.3

intercept respectively of the plots and are given in Table 5.

In comparison to the blank solution, the value of enthalpy of activation (ΔH^*) increased in the presence of EG and further increased when EG was added to anise extract. This result suggest that the corrosion reaction requires high energy to occur in the presence of the extract in combination with EG and more so, the activated complex or transition state complex formed with a slower rate in this inhibiting system. Inspection of the data in Table 5, reveals that ΔS^* values in the presence of the additives are more than that of the uninhibited solution and again is found to be more pronounced in anise extract + EG inhibiting system compared to EG alone. Both ΔH^* and ΔS^* values are positive in the absence and presence of the additives. The positive ΔH^* indicates the endothermic nature of the steel dissolution process whereas that of the ΔS^* suggests that active complexes were formed by the substitution of water the inhibitor [34, 35].

3.6. Explanation for Inhibition Mechanism

It is now known that anise extract and ethylene glycol provide inhibition to carbon steel corrosion in CO_2 saturated brine solution; however, the characteristic of the constituents that provide the inhibition is still unclear. To identify the probable constituents responsible for the inhibition, the chemical composition of the extract was studied by use of gas chromatography and mass spectrometry (GC–MS). The analysis of anise seeds extract, obtained by hydro distillation, using Gas Chromatography (GC) and Gas Chromatography/Mass Spectrometry (GC/MS) showed that the major components were trans-anethole (81.4.0%), limonene (6.50%), chavicol (2.10%), and anisaldehyde (1.81%) [36]. The molecular structure of trans-anethol is shown in Fig. 8. As can be seen, anethole is the major components among the other anise constituents. It can form complex compounds and also shows good oxygen scavenging characteristic. Thus, the mechanism of corrosion inhibition of carbon steel in CO_2 saturated brine solution by the phytochemicals of the extract can be explained on the basis of adsorption on the metal surface. This indicates that the *IE* of the extract is due to the presence of some or all the above listed phytochemical constituents. The adsorption of the inhibitor molecules on the carbon steel surface is due to the donor – acceptor interaction between π electrons of donor atoms O and aromatic rings of inhibitors and the acceptor, i.e. vacant d orbital of iron surface atoms [37]. The inhibitor molecules can also be adsorbed on the metal surface in the form of negatively charged species which can interact electrostatically with positively charged metal surface, which led to increase the surface coverage and consequently pro-

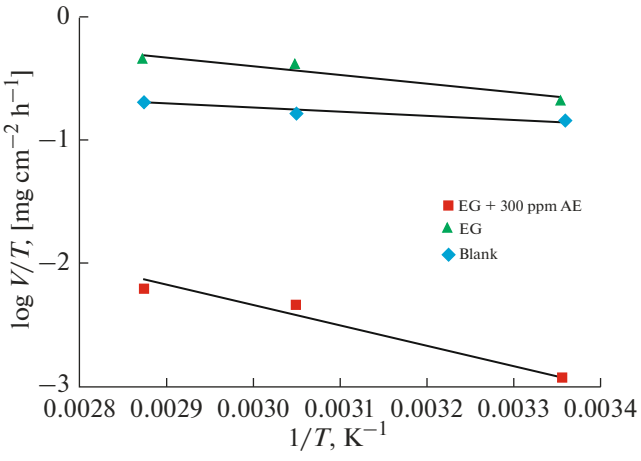

Fig. 7. Transition-state plots of log(V/T) versus $1/T$ in CO_2-saturated brine solution in absence and presence of various concentrations of AE.

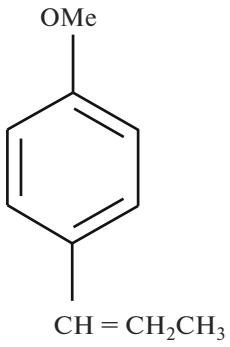

Fig. 8. Molecular structure of main component in anise extract.

tect efficiency even in the case of low inhibitor concentration.

Due to the two hydroxyl groups, glycol is a highly structured and water-like liquid [38]. It is fully miscible with water at room temperature. The auto-protolysis constant of EG solutions pK_{ap} remains close to 14, much like water, indicating that aqueous acid-base equilibria dominate. The experimental findings for physiochemical properties of water-glycol solutions showed which could influence the corrosion rate [18]. The solution viscosity increases strongly with increasing glycol concentration, and the diffusivity of CO_2 accordingly decreases. The increase of IE with temperature is explained with the change in the adsorption character: it is physical at a low temperature and transforms into chemical with its increase [39] and specific interaction between the inhibitor molecule and the carbon steel surface [40]. Hence it can be suggested that molecules of EG adsorb and block an essential part of the active sites on the carbon steel surface with forming strong chemisorption bonds.

3.7. AFM Surface Morphology

The surface morphologies of carbon steel specimens immersed in different test solutions were studied using atomic force microscope (AFM). AFM is ideally suited for characterization of the surface roughness of the metal specimens on a micro scale. The 3D and 2D images obtained after 24 h of immersion are presented in parts a–c of Fig. 9. It is observed that the carbon steel surface in 3.0% NaCl solution saturated with CO_2 is very rough. This rough surface is due to the rapid corrosion of the mild steel in 3.0% NaCl solution saturated with CO_2. However, in the presence of the EG and EG–AE mixtures, the carbon steel surface roughness was significantly reduced indicating the corrosion inhibition effect of the additives with more pronounced effect noticed with EG-AE mixtures. From

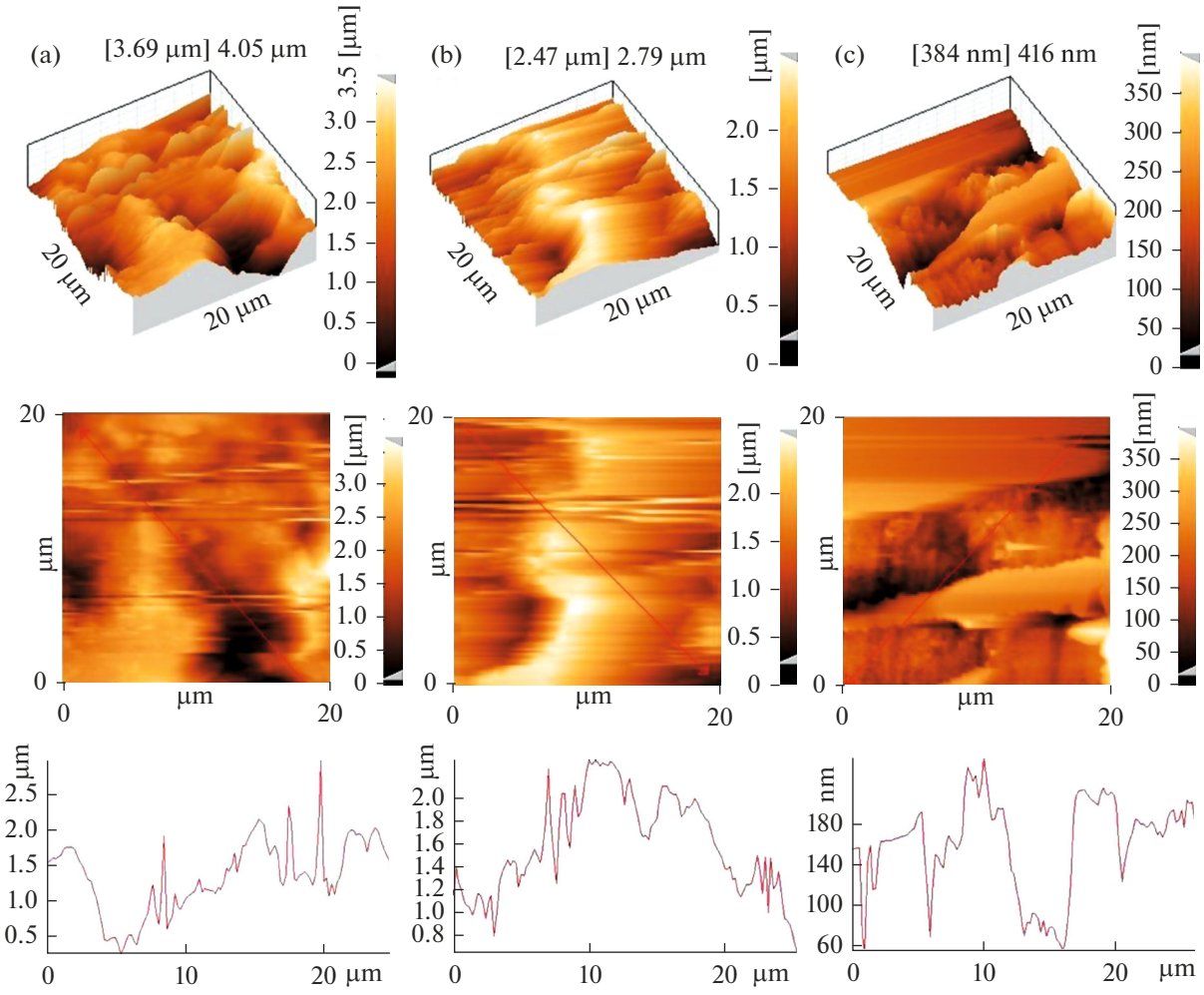

Fig. 9. Three and two-dimensional AFM images for exposed CK10 in (a) 3.0% NaCl solution saturated with CO_2, (b) 3.0% NaCl solution saturated with CO_2 containing 5 mL EG and (c) 3.0% NaCl solution saturated with CO_2 containing 5 mL EG + 300 ppm AE at 75°C for 24 h.

the 3D AFM images, the average roughness could not be read for the blank solution because of too rough surface. In the presence of the EG the average roughness was reduced to 2.79 μm. Addition of AE to EG further reduces the average roughness to 416 nm. The surface morphology results obtained on addition of anise extract to the EG are in agreement with the results obtained from electrochemical impedance spectroscopy and potentiodynamic polarization measurements and points to the existence of synergistic behavior of the anise extract compounds in combination with ethylene glycol.

4. CONCLUSIONS

Anise extract (AE) dissolved in ethylene glycol (EG) has been evaluated for its ability to reduce corrosion damage of CK10 carbon steel in CO_2-saturated brine, and from the results obtained the following conclusions can be drawn:

1. Anise extract dissolved in EG inhibited the corrosion of CK10 carbon steel in CO_2-saturated 3% NaCl solution and the extent of inhibition was found to be dependent on AE concentration.

2. Potentiodynamic polarization results revealed that the extract acts as a mixed-type corrosion inhibitor affecting both anodic metal dissolution and cathodic hydrogen evolution/oxygen reduction reactions.

3. The corrosion inhibition of the carbon steel was afforded by the adsorption of AE on the metal surface following the Langmuir adsorption isotherm model.

4. Impedance spectra show a high frequency capacitive loop related to the charge-transfer process of the metal corrosion and the double layer behavior. The EIS spectra are well fitted to the proposed structural model of the interface carbon steel/CO_2-saturated 3% NaCl + AE.

5. The AFM surface analysis confirmed the adsorption of the extract on the carbon steel surface leading to the reduction in the surface roughness in presence of anise extract in comparison to the one in uninhibited solution.

ACKNOWLEDGMENTS

This research has been supported financially by Najafabad Branch, Islamic Azad University.

REFERENCES

1. Ramesh Babu, B., *Anti-Corros. Methods Mater.,* 2005, vol. 52, p. 219.
2. Fouda, A.S., Mostafa, H.A., Heakal, F.E., and Elewady, G.Y., *Corros. Sci.,* 2005, vol. 47, p. 1988.
3. Zhang, S.T., Tao, Z.H., Li, W.H., and Hou, B.R., *Appl. Surf. Sci.,* 2009, vol. 255, p. 6757.
4. Li, D.G., Feng, Y.R., Bai, Z.Q., and Zheng, M.S., *Appl. Surf. Sci.,* 2007, vol. 253, p. 8371.
5. Nesic, S., Postlethwaite, J., and Olsen, S., *Corrosion,* 1996, vol. 52, p. 280.
6. Lopez, D.A., Simison, S.N., and de Sanchez, S.R., *Corros. Sci.,* 2005, vol. 47, p. 735.
7. Bilkova, K. and Gulbrandsen, E., *Electrochim. Acta,* 2008, vol. 53, p. 5423.
8. Kermani, M.B. and Morshed, A., *Corrosion,* 2003, vol. 59, p. 659.
9. El-Etre, A.Y. and Abdallah, M., *Corros. Sci.,* 2000, vol. 42, p. 731.
10. Lopez, D.A., Schreiner, W.H., de Sanchez, S.R., and Simison, S.N., *Appl. Surf. Sci.,* 2003, vol. 207, p. 69.
11. Zhang, G., Chen, C., Lu, M., et al., *Mater. Chem. Phys.,* 2007, vol. 105, p. 331.
12. Fouda, A.S., Rashwan, S.M., and Abo-Mosallam, H.A., *Desalin. Water Treat.,* 2013, vol. 1.
13. Okafor, P.C., Ikpi, M.E., Uwah, I.E., et al., *Corros. Sci.,* 2008, vol. 50, p. 2310.
14. Singh, A., Liu, Y., Liu, W., et al., *Int. J. Electrochem. Sci.,* 2013, vol. 8, p. 12884.
15. Zargari, A., *Medical Plants 2,* Tehran: Tehran Univ., 1989.
16. Hänsel, R., Sticher, O., and Steinegger, E., *Pharmakognosie-Phytopharmazie,* Berlin: Springer, 1999, p. 692.
17. Motalebi, A., Nasr-Esfahani, M., Ali, R., and Pourriahi, M., *Prog. Nat. Sci.,* 2012, vol. 22, p. 392.
18. Gulbrandsen, E. and Morard, J.H., *Corrosion,* 1998, vol. 98, no. 221.
19. Méndez, C., Singer, M., Camacho, A., et al., *Corrosion,* 2005, no. 5278.
20. Liu, F.G., Du, M., Zhang, J., and Qiu, M., *Corros. Sci.,* 2009, vol. 51, p. 102.
21. Okafor, P.C., Liu, X., and Zheng, Y.G., *Corros. Sci.,* 2009, vol. 51, p. 761.
22. Altoé, P., Pimenta, G., Moulin, C.F., et al., *Electrochim. Acta,* 1996, vol. 41, p. 1165.
23. López, D.A., Simson, S.N., and de Sánchez, S.R., *Corros. Sci.,* 2005, vol. 47, p. 735.
24. Zhang, G.A. and Cheng, Y.F., *Corros. Sci.,* 2009, vol. 51, p. 87.
25. Okafor, P.C., Liu, C.B., Liu, X., and Zheng, Y.G., *J. Solid State Electrochem.,* 2010, vol. 14, p. 1367.
26. Bouklah, M., Hammouti, B., Lagrenée, M., and Bentiss, F., *Corros. Sci.,* 2006, vol. 48, p. 2831.
27. Noor, E.A., *Int. J. Electrochem. Sci.,* 2007, vol. 2, p. 996.
28. Okafor, P.C., Ikpi, M.E., Uwah, I.E., et al., *Corros. Sci.,* 2008, vol. 50, p. 2310.
29. Nesic, S., *Corros. Sci.,* 2007, vol. 49, p. 4308.
30. West, J.M., *Basic Corrosion and Oxidation,* London: Ellis Horwood, 1980.
31. Ozcan, M., *J. Solid State Electrochem.,* 2008, vol. 12, p. 1653.
32. Desimone, M.P., Gordillo, G., and Simison, S.N., *Corros. Sci.,* 2011, vol. 53, p. 4033.

33. Putilova, I.N., Balezin, S.A., and Barannik, V.P., *Metallic Corrosion Inhibitors,* New York: Pergamon Press, 1960, p. 31.
34. Zou, C., Yan, X., Qin, Y., et al., *Corros. Sci.,* 2014, vol. 85, p. 445.
35. Tu, S., Jiang, X., Zhou, L., et al., *Corros. Sci.,* 2012, vol. 65, p. 13.
36. Gholivand, M.B., Rahimi-Nasrabadi, M., and Chalabi, H., *Anal. Lett.,* 2009, vol. 42, p. 1382.
37. Stern, M. and Geary, A.L., *J. Electrochem. Soc.,* 1957, vol. 104, p. 56.
38. Marcus, Y., *Pure Appl. Chem.,* 1990, vol. 62, p. 139.
39. Ivanov, E.S., *Ingibitory korrozii metallov v kislykh sredakh. Spravochnik (Inhibitors for Metal Corrosion in Acid Media. Handbook)*, Moscow: Metallurgiya, 1986.
40. Ammar, I.A. and El Khorafy, F.M., *Werkst. Korros.,* 1973, vol. 24, p. 702.